

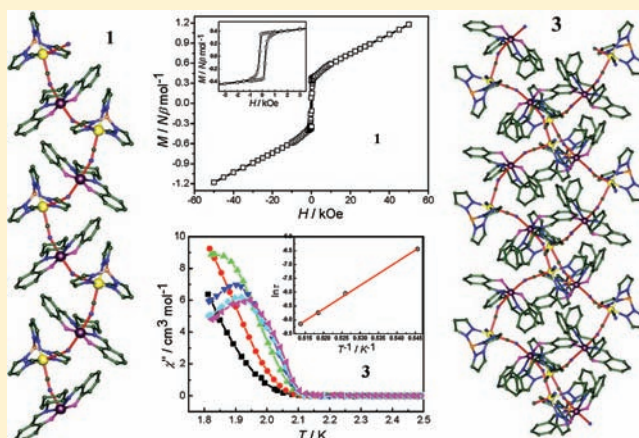
Chiral Cyanide-Bridged Cr^{III}–Mn^{III} Heterobimetallic Chains Based on [(Tp)Cr(CN)₃][−]: Synthesis, Structures, and Magnetic Properties

Min-Xia Yao, Qi Zheng, Xu-Min Cai, Yi-Zhi Li, You Song, and Jing-Lin Zuo*

State Key Laboratory of Coordination Chemistry, School of Chemistry and Chemical Engineering, Nanjing National Laboratory of Microstructures, Nanjing University, Nanjing 210093, P.R. China

Supporting Information

ABSTRACT: By the reactions of Mn^{III} Schiff-base complexes with the tricyanometalate building block, [(Tp)Cr(CN)₃][−] (Tp = Tris(pyrazolyl) hydroborate), two couples of enantiomerically pure chiral cyano-bridged heterobimetallic one-dimensional (1D) chain complexes, [Mn((R,R)-Salcy)Cr(Tp)(CN)₃·1/4H₂O·1/2CH₂Cl₂]_n (1) and [Mn((S,S)-Salcy)Cr(Tp)(CN)₃·1/4H₂O·1/2CH₂Cl₂]_n (2) (Salcy = *N,N'*-(1,2-cyclohexanediyethylene)bis(salicylideneiminato) dianion), [Mn((R,R)-Salphen)Cr(Tp)(CN)₃]_n (3) and [Mn((S,S)-Salphen)Cr(Tp)(CN)₃]_n (4) (Salphen = *N,N'*-1,2-diphenylethylene-bis(salicylideneiminato) dianion), have been successfully synthesized. Circular dichroism (CD) spectra confirm the enantiomeric nature of the optically active complexes. Structural analyses reveal the formation of neutral cyano-bridged zigzag single chains in 1 and 2, and neutral cyano-bridged zigzag double chains in 3 and 4. Magnetic studies show that antiferromagnetic couplings are operative between Cr^{III} and Mn^{III} centers bridged by cyanide. Complexes 1 and 2 are the rare examples of chiral ferrimagnets; while complexes 3 and 4 exhibit a coexistence of chirality and spin-glass behavior in a 1D chain.



INTRODUCTION

Molecule-based materials exhibiting interesting magnetic behaviors, which include magnetic ordering with high ordering/critical temperatures (T_c), single molecule/chain quantum effects, magnetic state switching control via photo, thermal, pressure, and so forth, have been one of hot topics because of their potential applications in magnetic devices.¹ Particularly, much attention has been focused on the rational design and construction of multifunctional magnetic materials, such as chiral magnets.^{2–7} It is expected that chiral magnets may exhibit a magneto-chiral dichroism (MChD) effect, magnetization induced second harmonic generation, or multiferroicity.^{3–7} Despite much effort, relatively few optically active magnetic complexes have been reported so far because of the difficulty of controlling chirality in the molecular structure as well as in the entire crystal structure.^{3–8} Moreover, rare success has been realized in molecule-based chiral magnets because of the challenge in the introduction of magnetic order and natural optical activity at a molecular level.^{4b,8} Single-chain magnets (SCMs) with slow magnetic relaxation below the blocking temperature are also attracting increasing interest owing to their unique properties and the potential use for high-density information storage.^{9,10} If chirality is introduced into SCMs, the new materials may behave as fascinating multifunctional

materials that combine the SCM behavior with other physical properties.^{3c,11,12}

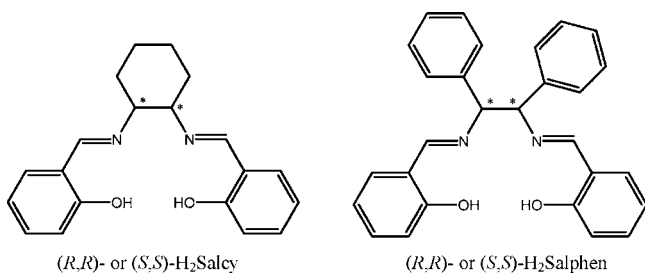
Recently, an effective strategy utilizing chiral multidentate ligands to interact paramagnetic carriers, such as transition metal ions and lanthanide ions, has been developed to prepare chiral magnetic compounds.^{4c,5b,13,14} In these studies, hexacyanometalates, octacyanometalates, or modified cyanometalates [(L)M(CN)_q]^{p−} anions (where L = polydentate N-donor chelating ligands; M = Cr, Fe, Mo, W, etc.) have been chosen as bridging units to coordinate unsaturated transition-metal complex [M'L*]^{m+} (L* = chiral coligands), yielding cyano-bridged chiral magnetic complexes.^{4a,8a–d,15,16} The short and conjugated linear cyanide can effectively mediate the magnetic interaction between two metal ions.¹⁷ Moreover, the topological structures of metal-cyanide complexes and the nature (ferromagnetic vs antiferromagnetic) of the metallic magnetic interactions can be easily controlled and anticipated.¹⁸ Following this strategy, with the use of [Fe^{III}(CN)₆]^{3−} or [(Tp)Fe^{III}(CN)₃][−], a series of chiral cyano-bridged chains and clusters that behave as ferrimagnets, SCMs, or single-molecule magnets (some of them showing the associated ferroelectricity) have been studied in our group.^{8a,11b,19}

Received: September 9, 2011

Published: February 3, 2012

Herein, we choose the tricyanometalate precursor, $[(\text{Tp})\text{Cr}(\text{CN})_3]^-$, as the bridging unit to construct new low dimensional chiral magnetic complexes. Aside from the virtue of good solubility and powerful coordinating ability, the chromium(III) ion in $[(\text{Tp})\text{Cr}(\text{CN})_3]^-$ has three unpaired electrons which can increase the strength of the magnetic exchange coupling.^{20,21} To fulfill the anisotropic demands for chiral magnetic complexes, the cationic manganese(III) chiral Schiff-base compound (Scheme 1) was introduced as the Lewis acid

Scheme 1. Chiral Schiff Base Ligands Used in This Work



(which has strong uniaxial anisotropy because of the Jahn–Teller effect of the six-coordinated Mn^{III} cation).²² In this paper, four enantiomerically pure chiral cyano-bridged heterobimetallic chain coordination polymers, $[\text{Mn}((R,R)\text{-Salcy})\text{Cr}(\text{Tp})(\text{CN})_3 \cdot 1/4\text{H}_2\text{O} \cdot 1/2\text{CH}_2\text{Cl}_2]_n$ (**1**) and $[\text{Mn}((S,S)\text{-Salcy})\text{Cr}(\text{Tp})(\text{CN})_3 \cdot 1/4\text{H}_2\text{O} \cdot 1/2\text{CH}_2\text{Cl}_2]_n$ (**2**), $[\text{Mn}((R,R)\text{-Salphen})\text{Cr}(\text{Tp})(\text{CN})_3]_n$ (**3**) and $[\text{Mn}((S,S)\text{-Salphen})\text{Cr}(\text{Tp})(\text{CN})_3]_n$ (**4**), have been synthesized. Their crystal structures, CD spectra, and magnetic properties are described.

$[(\text{Tp})\text{Cr}(\text{CN})_3]_n$ (**4**), have been synthesized. Their crystal structures, CD spectra, and magnetic properties are described.

EXPERIMENTAL SECTION

Starting Materials. All the reagents were commercially available and used without further purification. $(n\text{-Bu}_4\text{N})[(\text{Tp})\text{Cr}(\text{CN})_3]$ (Bu_4N^+ = tetrabutylammonium cation) was prepared according to the literature method.²⁰ The tetradentate Schiff base ligands, (R,R) - and (S,S) - H_2Salcy and (R,R) - and (S,S) - $\text{H}_2\text{Salphen}$ (Scheme 1), were synthesized from the condensation of salicylaldehyde with 1,2-diaminocyclohexane or 1,2-diphenylethylenediamine in a molar ratio of 2:1 in ethanol,²³ respectively.

Caution! Although no problems were encountered in this work, perchlorate salts are potentially explosive and cyanides are very toxic. Thus, these starting materials should be handled in small quantities and with great care.

Preparation of $[\text{Mn}(\text{SB})(\text{H}_2\text{O})_2](\text{ClO}_4)$. ($\text{SB} = (R,R)$ - and (S,S) - Salcy , and (R,R) - and (S,S) - Salphen , respectively). Similar to the method reported previously,²⁴ the manganese(III) precursors $[\text{Mn}(\text{SB})(\text{H}_2\text{O})_2]\text{ClO}_4$ were prepared by mixing $\text{Mn}(\text{OAc})_3 \cdot 2\text{H}_2\text{O}$, H_2SB , and NaClO_4 in methanol/ H_2O mixture with a molar ratio of 1:1:1.5.

Preparation of $[\text{Mn}((R,R)\text{-Salcy})\text{Cr}(\text{Tp})(\text{CN})_3 \cdot 1/4\text{H}_2\text{O} \cdot 1/2\text{CH}_2\text{Cl}_2]_n$ (1**).** A solution of $(n\text{-Bu}_4\text{N})[(\text{Tp})\text{Cr}(\text{CN})_3]$ (24.0 mg, 0.04 mmol) in dichloromethane/acetonitrile ($v/v = 3:1$) (10 mL) was added to a solution of $[\text{Mn}((R,R)\text{-Salcy})(\text{H}_2\text{O})_2]\text{ClO}_4$ (20.4 mg, 0.04 mmol) in 10 mL of dichloromethane/acetonitrile ($v/v = 3:1$). Slow evaporation of the resulting solution at room temperature yielded dark-brown rod-like crystals of **1** after a week. Yield: 75%. Anal. Calcd for $\text{C}_{32.5}\text{H}_{31.5}\text{BClCrMnN}_{11}\text{O}_{2.25}$: C, 51.00; H, 4.15; N, 20.13. Found: C, 51.01; H, 4.17; N, 20.10. IR (KBr, cm^{-1}): 2218, 2148 (ν_{CN}).

Preparation of $[\text{Mn}((S,S)\text{-Salcy})\text{Cr}(\text{Tp})(\text{CN})_3 \cdot 1/4\text{H}_2\text{O} \cdot 1/2\text{CH}_2\text{Cl}_2]_n$ (2**).** Compound **2** was prepared as dark-brown rod-like crystals in a similar method to that of **1**, except that $[\text{Mn}((S,S)\text{-Salphen})\text{Cr}(\text{Tp})(\text{CN})_3]_n$ (**3**) and $[\text{Mn}((S,S)\text{-Salphen})\text{Cr}(\text{Tp})(\text{CN})_3]_n$ (**4**).

Table 1. Summary of Crystallographic Data for the Complexes 1–4

	1	2	3	4
formula	$\text{C}_{130}\text{H}_{126}\text{B}_4\text{Cl}_4\text{Cr}_4\text{Mn}_4\text{N}_{44}\text{O}_9$	$\text{C}_{130}\text{H}_{126}\text{B}_4\text{Cl}_4\text{Cr}_4\text{Mn}_4\text{N}_{44}\text{O}_9$	$\text{C}_{40}\text{H}_{32}\text{BCrMnN}_{11}\text{O}_2$	$\text{C}_{40}\text{H}_{32}\text{BCrMnN}_{11}\text{O}_2$
fw	3061.55	3061.55	816.52	816.52
crystal system	orthorhombic	orthorhombic	monoclinic	monoclinic
space group	$P2_12_12$	$P2_12_12$	$P2_1$	$P2_1$
a , Å	15.729(2)	15.708(3)	13.3709(17)	13.3781(9)
b , Å	25.025(3)	25.004(5)	14.1169(17)	14.1119(9)
c , Å	9.1759(12)	9.1688(18)	20.935(3)	20.8914(14)
α , deg	90.00	90.00	90.00	90.00
β , deg	90.00	90.00	92.279(2)	92.2290(10)
γ , deg	90.00	90.00	90.00	90.00
V , Å ³	3611.7(8)	3601.2(12)	3948.4(8)	3941.1(5)
Z	1	1	4	4
ρ_{calcd} , g cm^{-3}	1.408	1.412	1.374	1.376
T/K	291(2)	291(2)	291(2)	291(2)
μ , mm^{-1}	0.772	0.774	0.645	0.646
θ , deg	1.63 to 26.00	1.63 to 25.08	1.74 to 26.00	1.78 to 26.00
$F(000)$	1570	1570	1676	1676
index ranges	$-19 \leq h \leq 14$, $-30 \leq k \leq 28$, $-11 \leq l \leq 10$	$-17 \leq h \leq 18$, $-29 \leq k \leq 19$, $-10 \leq l \leq 10$	$-16 \leq h \leq 16$, $-17 \leq k \leq 17$, $-25 \leq l \leq 19$	$-14 \leq h \leq 16$, $-17 \leq k \leq 11$, $-25 \leq l \leq 25$
data/restraints/parameters	7072/0/452	6391/0/452	14167/0/1009	12001/0/1009
GOF (F^2)	1.070	1.073	1.063	1.020
R_1^a, wR_2^b ($I > 2\sigma(I)$)	0.0585 0.1031	0.0601 0.1121	0.0558 0.1150	0.0576 0.1230
R_1^a, wR_2^b (all data)	0.0802 0.1071	0.0764 0.1156	0.0787 0.1215	0.0768 0.1286
Flack χ	0.01(2)	0.01(2)	0.038(17)	0.019(19)

$$^a R_1 = \sum \|F_o\| - |F_c| / \sum \|F_o\|. \quad ^b wR_2 = [\sum w(F_o^2 - F_c^2)^2 / \sum w(F_o^2)]^{1/2}.$$

Table 2. Selected Bond Lengths (Å) and Angles (deg) for 1^a

C10—Cr1	2.058(5)	C11—Cr1	2.059(5)
C12—Cr1	2.058(5)	Cr1—N1	2.043(4)
Cr1—N5	2.051(4)	Cr1—N3	2.054(4)
Mn1—O1	1.866(3)	Mn1—O2	1.879(3)
Mn1—N11	1.977(4)	Mn1—N10	2.002(4)
Mn1—N7	2.295(4)	Mn1—N9	2.317(4)
N7—C10—Cr1	178.6(4)	N8—C11—Cr1	176.0(4)
N9 ^{#1} —C12—Cr1	173.9(4)	N1—Cr1—N5	85.73(16)
N1—Cr1—N3	87.62(15)	N5—Cr1—N3	86.84(15)
N1—Cr1—C10	91.24(17)	N5—Cr1—C10	175.58(17)
N3—Cr1—C10	89.83(16)	N1—Cr1—C12	88.69(17)
N5—Cr1—C12	90.03(16)	N3—Cr1—C12	175.32(17)
C10—Cr1—C12	93.12(17)	N1—Cr1—C11	177.5(2)
N5—Cr1—C11	91.96(19)	N3—Cr1—C11	93.11(17)
C10—Cr1—C11	91.1(2)	C12—Cr1—C11	90.47(18)
O1—Mn1—O2	95.00(13)	O1—Mn1—N11	92.29(14)
O2—Mn1—N11	172.18(16)	O1—Mn1—N10	173.84(14)
O2—Mn1—N10	91.01(14)	N11—Mn1—N10	81.65(15)
O1—Mn1—N7	93.80(14)	O2—Mn1—N7	90.86(15)
N11—Mn1—N7	85.83(15)	N10—Mn1—N7	84.73(15)
O1—Mn1—N9	93.50(15)	O2—Mn1—N9	89.01(15)
N11—Mn1—N9	93.38(15)	N10—Mn1—N9	87.96(15)
N7—Mn1—N9	172.68(15)	C10—N7—Mn1	160.2(4)
C12 ^{#2} —N9—Mn1	150.4(4)		

^aSymmetry transformations used to generate equivalent atoms are given in footnotes #1 to #2. ^{#1} $x-1/2, -y+3/2, -z+1$. ^{#2} $x+1/2, -y+3/2, -z+1$.

Table 3. Selected Bond Lengths (Å) and Angles (deg) for 3^a

C10—Cr1	2.022(5)	C11—Cr1	2.075(5)
C12—Cr1	2.050(5)	C69—Cr2	2.052(6)
C70—Cr2	2.057(6)	C71—Cr2	2.046(6)
Cr1—N6	2.048(4)	Cr1—N4	2.051(4)
Cr1—N2	2.087(4)	Cr2—N21	2.030(4)
Cr2—N19	2.032(4)	Cr2—N17	2.054(5)
Mn1—O1	1.874(3)	Mn1—O2	1.880(3)
Mn1—N10	1.978(3)	Mn1—N11	1.978(4)
Mn1—N9	2.318(4)	Mn1—N8	2.333(4)
Mn2—O4	1.873(3)	Mn2—O3	1.902(3)
Mn2—N13	2.012(4)	Mn2—N12	2.016(4)
Mn2—N15	2.240(6)	Mn2—N16	2.270(5)
N7—C10—Cr1	177.9(4)	N8—C11—Cr1	172.8(4)
N9 ^{#1} —C12—Cr1	175.9(4)	N14—C69—Cr2	174.1(5)
N15 ^{#2} —C70—Cr2	154.0(7)	N16—C71—Cr2	174.3(5)
C10—Cr1—N6	92.57(15)	C10—Cr1—C12	87.2(2)
N6—Cr1—C12	92.24(13)	C10—Cr1—N4	91.73(14)
N6—Cr1—N4	87.00(17)	C12—Cr1—N4	178.63(13)
N21—Cr2—N19	86.72(18)	N21—Cr2—C71	92.3(2)
N19—Cr2—C71	93.27(19)	N21—Cr2—C69	91.9(2)
N19—Cr2—C69	178.5(2)	C71—Cr2—C69	86.3(2)
N11—Mn1—N9	88.90(15)	O1—Mn1—N8	91.77(15)
O2—Mn1—N8	89.64(15)	N10—Mn1—N8	89.65(16)
N11—Mn1—N8	82.83(15)	N9—Mn1—N8	171.70(15)
N12—Mn2—N15	95.60(18)	O4—Mn2—N16	89.75(16)
O3—Mn2—N16	86.47(17)	N13—Mn2—N16	92.76(16)
N12—Mn2—N16	87.48(16)	N15—Mn2—N16	175.86(19)
C11—N8—Mn1	149.1(3)	C12 ^{#3} —N9—Mn1	158.5(3)
C70 ^{#4} —N15—Mn2	172.5(6)	C71—N16—Mn2	150.6(4)

^aSymmetry transformations used to generate equivalent atoms are given in footnotes #1 through #4. ^{#1} $-x+2, y+1/2, -z+2$. ^{#2} $-x+1, y-1/2, -z+1$. ^{#3} $-x+2, y-1/2, -z+2$. ^{#4} $-x+1, y+1/2, -z+1$.

Salcy)(H₂O)₂]ClO₄ was used. Yield: 72%. Anal. Calcd for C_{32.5}H_{31.5}BClCrMnN₁₁O_{2.25}: C, 51.00; H, 4.15; N, 20.13. Found: C, 51.02; H, 4.16; N, 21.12. IR (KBr, cm⁻¹): 2216, 2149 (ν_{CN}).

Preparation of [Mn((R,R)-Salphen)Cr(Tp)(CN)₃]_n (3). A solution of (*n*-Bu₄N)[(Tp)Cr(CN)₃] (24.0 mg, 0.04 mmol) in 4 mL of methanol was added to a solution of [Mn((R,R)-Salphen)(H₂O)₂]ClO₄ (24.4 mg, 0.04 mmol) in 6 mL of methanol. Slow evaporation of the resulting solution at room temperature gave dark-brown rod-like crystals of **3** after a week. Yield: 65%. Anal. Calcd for C₄₀H₃₂BCrMnN₁₁O₂: C, 58.84; H, 3.95; N, 18.87. Found: C, 58.87; H, 3.97; N, 18.86. IR (KBr, cm⁻¹): 2148 (ν_{CN}).

Preparation of [Mn((S,S)-Salphen)Cr(Tp)(CN)₃]_n (4). Compound **4** was prepared as dark-brown rod-like crystals in a similar method to that of **3**, except that [Mn((S,S)-Salphen)(H₂O)₂]ClO₄ was used. Yield: 68%. Anal. Calcd for C₆₆H₆₅B₂Fe₂Mn₂N₂₃O₅: C, 58.84; H, 3.95; N, 18.87. Found: C, 58.86; H, 3.97; N, 18.85. IR (KBr, cm⁻¹): 2149 (ν_{CN}).

X-ray Structure Determination. The crystal structures were determined on a Siemens (Bruker) SMART CCD diffractometer using monochromated Mo K α radiation ($\lambda = 0.71073$ Å) at 291 K. Cell parameters were retrieved using SMART software and refined using SAINT²⁵ on all observed reflections. Data was collected using a narrow-frame method with scan widths of 0.30° in ω and an exposure time of 10 s/frame. The highly redundant data sets were reduced using SAINT²⁵ and corrected for Lorentz and polarization effects. Absorption corrections were applied using SADABS²⁶ supplied by Bruker. Structures were solved by direct methods using the program SHELXL-97.²⁷ The positions of the metal atoms and their first coordination spheres were located from direct-methods *E* maps; other non-hydrogen atoms were found in alternating difference Fourier syntheses and least-squares refinement cycles and, during the final cycles, refined anisotropically. Hydrogen atoms were placed in calculated positions and refined as riding atoms with a uniform value of U_{iso} which are tied 1.2 times or 1.5 times (for methyl-group) to the parent atoms. Final crystallographic data and values of R_1 and wR_2 are listed in Table 1. Selected bond distances and angles for complexes **1–4** are listed in Tables 2, Supporting Information, Table S1, Table 3 and Supporting Information, Table S2, respectively.

Physical Measurements. Elemental analyses for C, H, and N were performed on a Perkin-Elmer 240C analyzer. Infrared spectra were recorded on a Vector22 Bruker Spectrophotometer with KBr pellets in the 400–4000 cm⁻¹ region. The circular dichroism spectra were recorded on a JASCO J-810 Spectropolarimeter with KBr pellets. The ferroelectric property of the solid-state sample was measured as the pellet-covered silver-conductive glue on the Radiant Technologies Premier Precision II ferroelectric tester at room temperature. Magnetic susceptibilities for all polycrystalline samples were measured with the use of a Quantum Design MPMS-XL7 SQUID magnetometer in the temperature range 1.8–300 K. Field dependences of magnetization were measured using Quantum Design MPMS-XL5 SQUID system in an applied field up to 50 kOe.

RESULTS AND DISCUSSION

Spectroscopic and Ferroelectric Studies. Circular dichroism (CD) spectra measured in KBr pellets confirm the enantiomeric nature of the optically active complexes **1–4** (Figure 1a,b). The CD spectrum of **1** (*R* isomer) exhibits a negative Cotton effect at $\lambda_{\text{max}} = 358, 400,$ and 463 nm, while **2** (*S* isomer) shows Cotton effects of the opposite sign at the same wavelengths. Complex **3** (*R* isomer) exhibits a negative Cotton effect at $\lambda_{\text{max}} = 326$ nm, while **4** (*S* isomer) also shows Cotton effect of the opposite sign at the same wavelength.

Given that complexes **1–4** crystallize in a chiral space group, their second-order nonlinear optical properties were studied. The results from the powdered sample indicate that **1–4** show second-order NLO effect with approximate responses of 0.4 times that of urea. Although **3** and **4** crystallize in a polar point

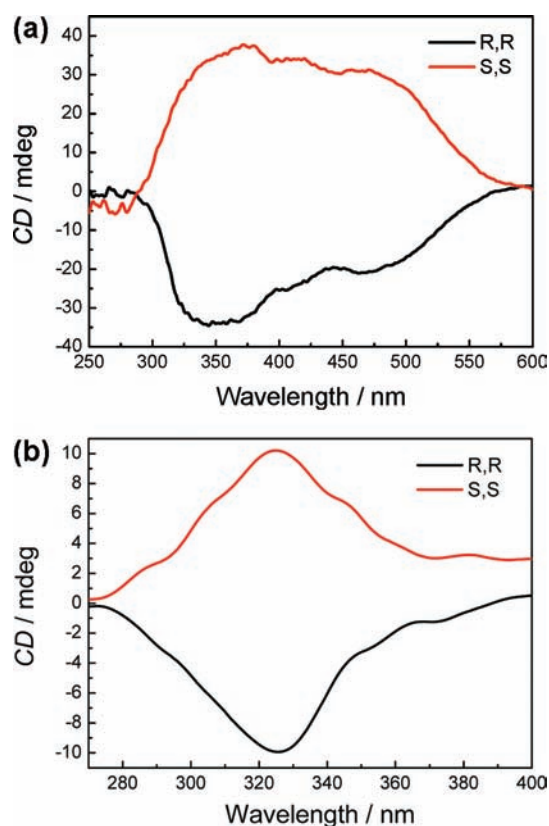


Figure 1. (a) CD spectra of **1** (*R,R* isomer, black) and **2** (*S,S* isomer, red) in KBr pellets. (b) CD spectra of **3** (*R,R* isomer, black) and **4** (*S,S* isomer, red) in KBr pellets.

group (C_2) required for ferroelectric behavior, no ferroelectric properties are observed for them at room temperature.

Structural Description. Complexes **1** and **2** are a pair of enantiomers. Both compounds show similar crystal structures, and they are crystallized in the chiral space group $P2_12_12$ (Figure 2). They are made up of a neutral cyano-bridged zigzag chain with $(-\text{Cr}-\text{C}\equiv\text{N}-\text{Mn}-\text{N}\equiv\text{C}-)_n$ as the repeating unit. Here, only the crystal structure of **1** is described in detail (Figure 3). Within the chain, each $[(\text{Tp})\text{Cr}(\text{CN})_3]^-$ entity acts as a bidentate ligand toward the $[\text{Mn}((R,R)\text{-Salcy})]^+$ motifs through two of its three cyanide groups in cis positions, whereas each $[\text{Mn}((R,R)\text{-Salcy})]^+$ unit is linked to two $[\text{TpCr}(\text{CN})_3]^-$ ions in trans modes. The Cr(III) ion possesses a slightly distorted octahedral coordination environment, coordinated by three carbon atoms from cyanide groups and three nitrogen atoms from different pyrazolyl groups. The Cr^{III}–C(cyano) (2.058(5)–2.059(5) Å) and Cr^{III}–N(pyrazole) (2.043(4)–2.054(4) Å) bond lengths are in good agreement with those observed previously in related compounds.²⁰ The Cr–C \equiv N angles for both terminal (176.0(4)°) and bridging (173.9(4) and 178.6(4)°) cyanide groups depart slightly from linearity. In the $[\text{Mn}((R,R)\text{-Salcy})]^+$ unit, the Mn(III) ion situates in an obviously distorted octahedral geometry based on equatorial N₂O₂ donor atoms from (*R,R*)-Salcy (Mn1–O1 = 1.866(3) Å, Mn1–O2 = 1.879(3) Å, Mn1–N10 = 2.002(4) Å, and Mn1–N11 = 1.977(4) Å) and two apical N atoms from bridging CN groups (Mn1–N7 = 2.295(4) Å and Mn1–N9 = 2.317(4) Å). These values agree with those observed in other complexes including high-spin $[\text{Mn}^{\text{III}}(\text{SB})]^{n+}$ species.^{8a,18c,22a,28,29} The axial elongation results from the well-

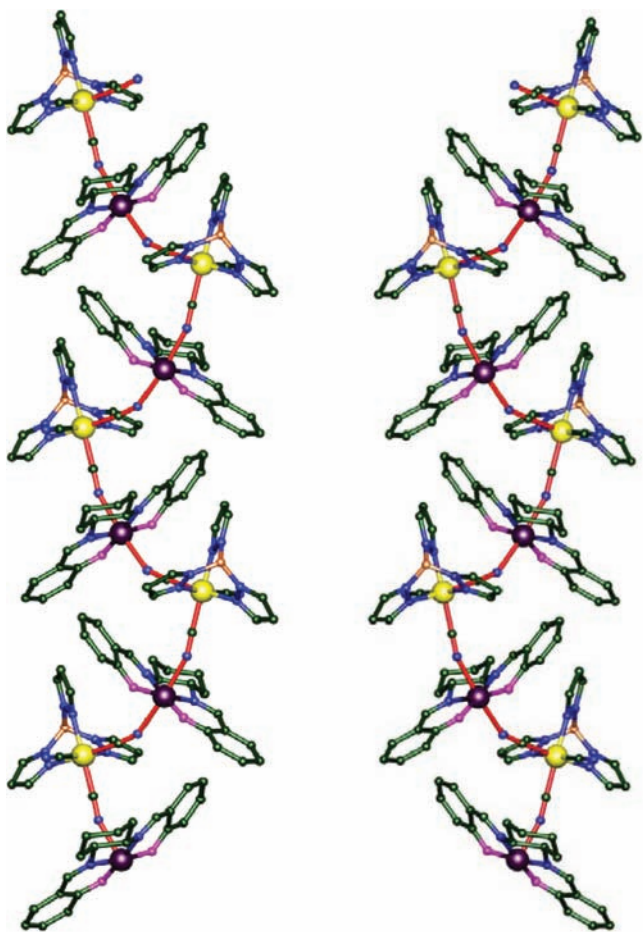


Figure 2. Perspective view of one-dimensional zigzag infinite chains of **1** (*R,R* isomer, left) and **2** (*S,S* isomer, right), respectively.

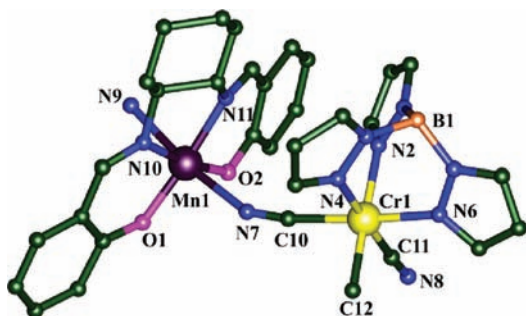


Figure 3. Perspective drawing of the crystallographically structural unit of **1** showing the atom numbering. H atoms are omitted for clarity.

known Jahn–Teller effect on an octahedral high-spin Mn(III) ion.²² The Mn–N≡C bond angles deviate significantly from linearity with the angles of Mn1–N7–C10 = 160.2(4)° and Mn1–N9–C12#2 = 150.4(4)° (symmetric operation: #2: $x + 1/2, -y + 3/2, -z + 1$). The shorter intrachain Cr⋯Mn distances through the cyanide bridges are 5.299 Å for Cr1–Mn1, and 5.413 Å for Cr1–Mn1#2. The shortest interchain Cr⋯Mn, Mn⋯Mn, and Cr⋯Cr distances are 8.266, 9.176, and 9.176 Å, respectively. Each chain interacts with two other adjacent chains by the O–H⋯N interactions between the solvated water molecules and the nonbridged cyanide groups (the O⋯N separation: 3.491 Å), and the weak B–H⋯Cl interactions between the solvated CH₂Cl₂ molecules and

pyrazole ligands (the B⋯Cl separation: 3.845 Å), thus forming a two-dimensional (2D) layer (Supporting Information, Figure S1). The layers stack into a three-dimensional (3D) structure along the *c* axis via weak H-bonding interactions (Supporting Information, Figure S2).

Complexes **3** and **4** are also enantiomers but crystallize in chiral space group *P*2₁. They are made up of neutral cyano-bridged zigzag double chains with (–Cr–C≡N–Mn–N≡C–)_{*n*}, as the repeating unit (Figure 4); no detailed descriptions

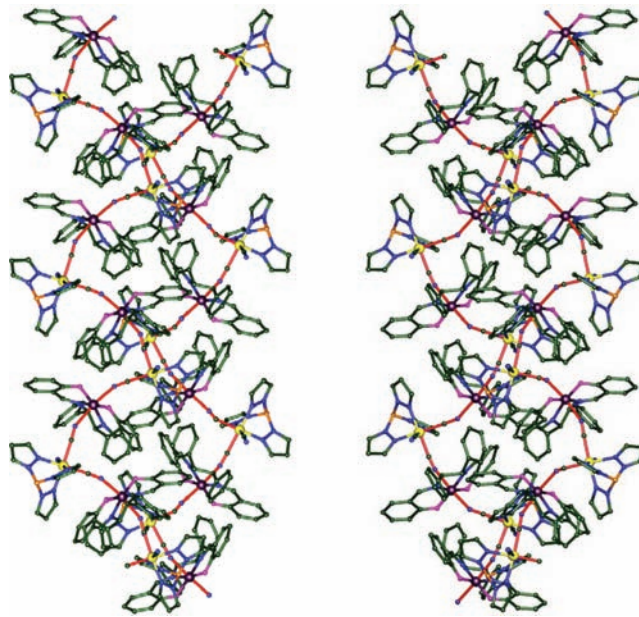


Figure 4. Perspective view of 1D zigzag infinite chains of **3** (*R,R* isomer, left) and **4** (*S,S* isomer, right), respectively.

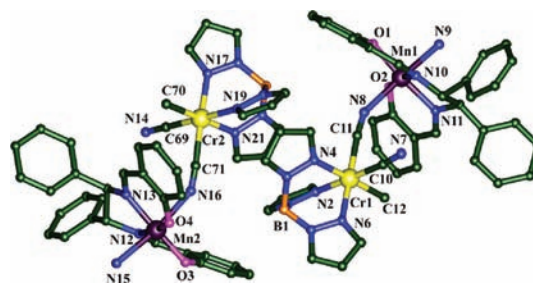


Figure 5. Perspective drawing of the crystallographically structural unit of **3** showing the atom numbering. H atoms are omitted for clarity.

are presented here for **4**. As shown in Figure 5, in complex **3**, the crystallographically independent unit contains two types of [(Tp)Cr(CN)₃][–] anions (including Cr1 and Cr2 atoms, respectively). Both Cr1 and Cr2 ions possess a slightly distorted octahedral coordination environment, and the Cr^{III}–C(cyano) (2.022(5)–2.075(5) Å) and Cr^{III}–N(pyrazole) (2.030(4)–2.087(4) Å) bond lengths are within the normal values.²⁰ The Cr1–C≡N angles (172.8(4)–176.8(4)°) show only slight deviation from linearity, while the Cr2–C≡N angles (154.0(7)–174.3(5)°) deviate more from linearity. There are also two crystallographically independent Mn(III) ions in complex **3**, Mn1 and Mn2. Both Mn(III) ions have an obviously distorted octahedral geometry with the equatorial

plane occupied by N_2O_2 atoms from the (*R,R*)-Salphen ligand and the two axial positions occupied by two cyanide nitrogen atoms. Because of the Jahn–Teller distortion of the Mn(III) ions, the axial bond lengths (2.318(4) Å and 2.333(4) Å for Mn1, 2.240(6) Å and 2.270(5) Å for Mn2) are relatively longer than the equatorial ones (1.874(3)–1.978(4) Å for Mn1 and 1.873(3)–2.016(4) Å for Mn2), but comparable to those of $[\text{Cr}^{\text{III}}(\text{AA})(\text{CN})_4]^-$ (AA = α -diimine type ligands).^{28d,29h} The Mn–N \equiv C bonds deviate significantly from linearity with the Mn1–N \equiv C bonds (149.1(3) and 158.5(3)°) and the Mn2–N \equiv C bonds (150.6(4) and 172.5(6)°), which are similar to the cyanide-linked $\text{Fe}^{\text{III}}\text{–Mn}^{\text{III}}$ chain containing the facial $[\text{Fe}(\text{Tp})(\text{CN})_3]^-$ anion.^{28e} The Cr1 and Mn1 atoms are linked by cyanide to form 1D infinite chain along the *b* axis, and the Cr2 and Mn2 atoms are also linked by cyanide to form another 1D infinite chain in the same way. The chains repeat in an ...ABAB... stacking sequence (Supporting Information, Figure S3). The shorter intrachain Cr–Mn distances are 5.290 Å for Cr1–Mn1 and 5.379 Å for Cr1–Mn1#1, 5.225 Å for Cr2–Mn2 and 5.100 Å for Cr2–Mn2#2 (symmetric operation: #1: $-x+2, y+1/2, -z+2$; #2: $-x+1, y-1/2, -z+1$), respectively. The shortest interchain Cr...Cr, Mn...Mn, and Cr...Mn distances are 8.033, 11.936, and 8.892 Å, respectively.

Magnetic Properties. Magnetic susceptibility measurements were performed on polycrystalline samples of complexes 1–4 using the SQUID magnetometer at temperatures ranging from 1.8 to 300 K.

The temperature dependence of the $\chi_{\text{M}}T$ values of 1 under 2 kOe is displayed in Figure 6. The $\chi_{\text{M}}T$ value per $\text{Cr}^{\text{III}}\text{Mn}^{\text{III}}$ unit

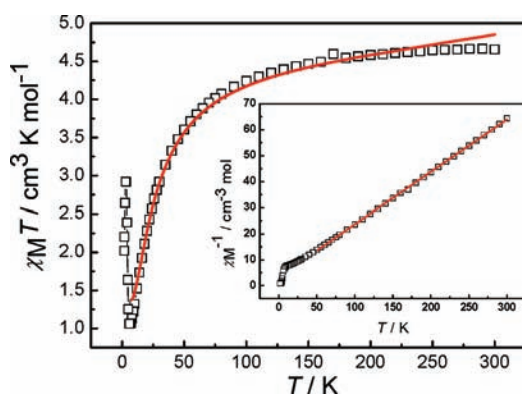


Figure 6. Temperature dependence of the $\chi_{\text{M}}T$ product for 1 at 2 kOe. The red solid line represents the best fits of the data. Inset: Plot of $1/\chi_{\text{M}}$ vs T . The red solid line is the fitting result by Curie–Weiss law.

at 300 K is $4.66 \text{ cm}^3 \cdot \text{K} \cdot \text{mol}^{-1}$, which is close to the value of $4.88 \text{ cm}^3 \cdot \text{K} \cdot \text{mol}^{-1}$ expected for one spin-only Cr(III) center ($S = 3/2$) and one Mn(III) center ($S = 2$) assuming $g = 2.00$ and no exchange coupling. Upon cooling, the $\chi_{\text{M}}T$ values decrease very smoothly down $4.24 \text{ cm}^3 \cdot \text{K} \cdot \text{mol}^{-1}$ at 100 K and then more steeply, reaching $1.06 \text{ cm}^3 \cdot \text{K} \cdot \text{mol}^{-1}$ at 6 K. Upon further cooling, the $\chi_{\text{M}}T$ value abruptly increases to a maximum value of $2.92 \text{ cm}^3 \cdot \text{K} \cdot \text{mol}^{-1}$ at about 3 K. It indicates the presence of intrachain antiferromagnetic coupling between neighboring Cr^{III} and Mn^{III} ions. Eventually, a drastic drop occurs until the value of $2.02 \text{ cm}^3 \cdot \text{K} \cdot \text{mol}^{-1}$ at 1.8 K, which may be relevant to zero field splitting and/or Zeeman effects. The magnetic susceptibility above 50 K obeys the Curie–Weiss law with $C = 4.96 \text{ cm}^3 \cdot \text{K} \cdot \text{mol}^{-1}$ and a Weiss constant $\theta = -17.34 \text{ K}$ (inset of Figure 6). The negative θ indicates dominant antiferromagnetic

(AF) coupling in 1, which is consistent with other cyanide-bridged Cr/Mn compounds.^{28d,29b,h,30} Since the chains possess two kinds of CN^- bridges with different bond geometries, the two unique couplings along the chain should be of different magnitudes. A regular chain model is not suitable for evaluating the intrachain couplings. As a consequence, the alternating ferrimagnetic chain model was used.³¹ The spin Hamiltonian is $H = -J \sum_i S_{\text{Cr}^{\text{III}}} \cdot [(1 + \alpha)S_{\text{Mn}^{\text{III}}} + (1 - \alpha)S_{\text{Mn}^{\text{III}}+1}]$, where the local spins are S_{Cr} and S_{Mn} , the local Zeeman factors g_{Cr} and g_{Mn} , and the couplings between nearest neighbors $J(1 + \alpha)$ and $J(1 - \alpha)$. The best fit between 8.0 and 300 K gives $g_{\text{Mn}} = 1.95$, $g_{\text{Cr}} = 2.03$, $J = -1.95 \text{ cm}^{-1}$, $\alpha = 0.30$ and $zJ' = 0.51 \text{ cm}^{-1}$ ($R = 7.23 \times 10^{-3}$). The J value denotes that weak antiferromagnetic couplings between Cr^{III} and Mn^{III} ions within a chain are operating.

To investigate the phase transformation at low temperature, the field-cooled (FC) and zero-field-cooled (ZFC) magnetization measurements were performed for 1 at 10 Oe in the 1.8–10 K. Both ZFC and FC curves show abrupt increases below 4.0 K and have a divergence, suggesting the occurrence of the long-range magnetic ordering below this temperature (Figure 7). To further probe the long-range ordering in 1, the

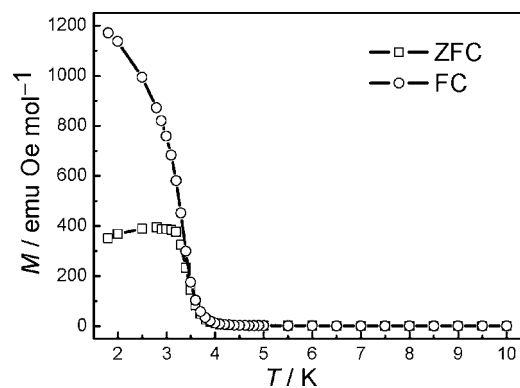


Figure 7. Temperature dependence of magnetization for 1 at 10 Oe: ZFC (\square) and FC (\circ) magnetization.

measurements of alternating current (ac) magnetic susceptibilities were carried out at zero direct current (dc) field (Figure 8). There is a peak in the in-phase (χ_{M}') signal and in the out-of-phase (χ_{M}'') signal at 3.8 K, respectively, indicating the occurrence of a magnetic phase transition at this temperature. No frequency dependence was observed for the peak positions of χ_{M}' and χ_{M}'' , thus precluding the single chain magnetic behavior for 1. Furthermore, a characteristic hysteresis loop is observed at 1.8 K with a remnant magnetization (M_r) of 0.36 $N\beta$ and a coercive field (H_c) of 240 Oe (Figure 9), indicating a soft magnet behavior of 1.

Complex 2 shows the same magnetic behavior as that of complex 1 (Supporting Information, Figures S4–S7). A pure 1D system cannot create a long-range magnetic ordering at $T > 0 \text{ K}$.³¹ However, in 1 and 2, there are weak interchain interactions to form a 2D supramolecular array as described above, and they may play an important role in their long-range magnetic ordering.³²

Compared with $[\text{Mn}((R,R)\text{-Salcy})\text{Fe}(\text{Tp})(\text{CN})_3 \cdot \text{H}_2\text{O} \cdot 1/2\text{CH}_3\text{CN}]_n$ and $[\text{Mn}((S,S)\text{-Salcy})\text{Fe}(\text{Tp})(\text{CN})_3 \cdot \text{H}_2\text{O} \cdot 1/2\text{CH}_3\text{CN}]_n$, which display metamagnetic behavior from an anti-ferromagnetic phase to a ferromagnetic phase and exhibit an antiferromagnetic long-range ordering with a T_N of 3.2 K,³³

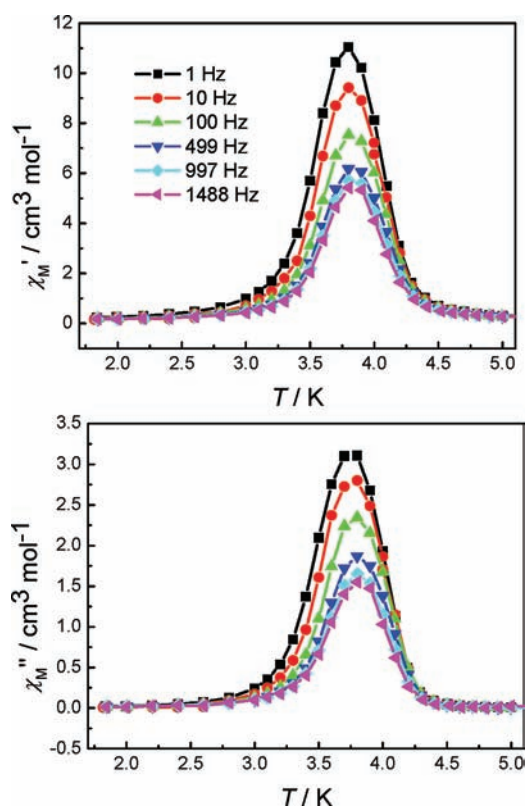


Figure 8. Temperature dependence of the in-phase χ' and out-of-phase χ'' at different frequencies in a 5 Oe ac field oscillating at 1–1488 Hz with a zero applied dc field for **1**.

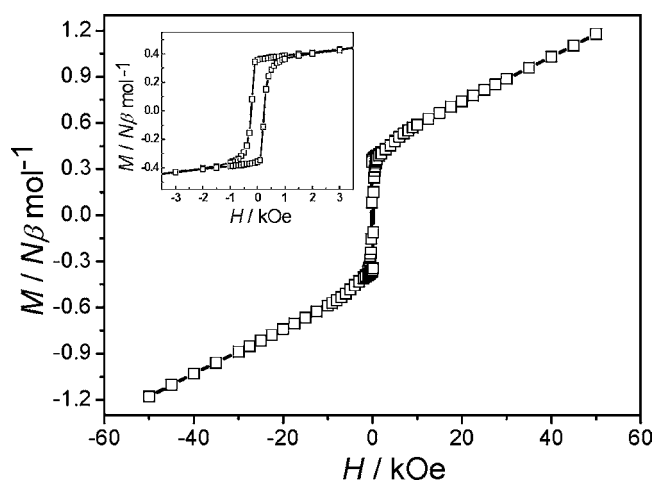


Figure 9. Hysteresis loop for **1** at 1.8 K. Inset: the zoomed hysteresis loop.

complexes **1** and **2** are ferrimagnets. It has been experimentally shown that the magnetic coupling between low-spin Fe(III) and high-spin Mn(III) is ferromagnetic arising from the strict orthogonality of the magnetic orbitals (t_{2g} in Fe^{III} vs d_{z^2} in Mn^{III}) or antiferromagnetic arising from the orbital overlap between them.³⁴ The overall magnetic property depends on which contribution is predominant. The Mn–N≡C bond angle may play an important role in controlling the magnetic coupling. However, the cyanide-bridged Cr(III)–Mn(III) complexes usually show antiferromagnetic coupling through the orbital overlap between t_{2g} orbitals of Cr^{III} and Mn^{III}.^{35,29h} As the Cr^{III} and Mn^{III} ions possess uncompensated spins, these

intrachain AF couplings together with the interchain ferromagnetic couplings produce the ferrimagnet for complexes **1** and **2**.

The magnetic susceptibility data for **3** were collected at 2 kOe, as plotted in Figure 10. At 300 K, the $\chi_M T$ value of 4.60

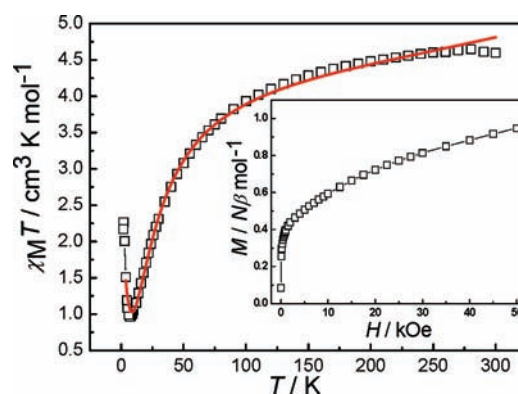


Figure 10. Temperature dependence of the $\chi_M T$ product for **3** at 2 kOe. The red solid line represents the best fits of the data. Inset: Field dependence of magnetization at 1.8 K.

$\text{cm}^3 \cdot \text{K} \cdot \text{mol}^{-1}$ is close to the expected value of $4.88 \text{ cm}^3 \cdot \text{K} \cdot \text{mol}^{-1}$ for one spin-only Cr(III) center ($S = 3/2$) and one Mn(III) center ($S = 2$) assuming $g = 2.00$ and no exchange coupling. Upon lowering the temperature, the $\chi_M T$ values decrease gradually to a minimum of $0.97 \text{ cm}^3 \cdot \text{K} \cdot \text{mol}^{-1}$ at 7.0 K, and then increase quickly to a maximum of $2.26 \text{ cm}^3 \cdot \text{K} \cdot \text{mol}^{-1}$ at 2.0 K. Upon further cooling, $\chi_M T$ drops sharply. It indicates the occurrence of intrachain antiferromagnetic coupling between Cr(III) and Mn(III) ions. The magnetic susceptibility follows the Curie–Weiss law above 50 K with $C = 5.17 \text{ cm}^3 \cdot \text{K} \cdot \text{mol}^{-1}$ and $\theta = -31.91 \text{ K}$, further confirming the presence of dominant antiferromagnetic couplings between neighboring Cr(III) and Mn(III) ions (Supporting Information, Figure S8). To gain further insight into the underlying magnetic nature in **3**, the field dependence of magnetization was measured at 1.8 K. There is a rapid increase from 0 to 2 kOe and then it increases more slowly to a maximum value of $0.95 N\beta$ at 50 kOe, which is close to the expected value of $1 N\beta$ with the antiferromagnetic coupling between Cr^{III} and Mn^{III} ions (inset of Figure 10). According to the structure data, the Cr^{III}–C≡N–Mn^{III} linkage is obviously different. So an alternating ferrimagnetic chain model was used.³¹ The susceptibility data were fitted using the same expression for complexes **1** and **2**, giving $g_{\text{Mn}} = 1.96$, $g_{\text{Cr}} = 1.99$, $J = -1.95 \text{ cm}^{-1}$, $\alpha = 0.40$ and $zJ' = 0.04 \text{ cm}^{-1}$ ($R = 4.81 \times 10^{-3}$). The fitting results imply there are weaker interchain couplings of **3** than those of **1** and **2**.

To investigate the dynamic nature, the ac susceptibility of complex **3** was measured in the frequency range 1–1488 Hz at 1.8–5.0 K (Figure 11). Both the in-phase (χ_M') and out-of-phase (χ_M'') susceptibility signals display obvious frequency-dependence below 2.1 K. The frequency dependence of the peak temperature shift (ΔT_p) of χ_M' is measured by a parameter $\phi = (\Delta T_p / T_p) / \Delta(\log f) = 0.02$, consistent with canonical spin-glass behavior.³⁶ Using the Arrhenius equation $\tau = \tau_0 \exp(\Delta / k_B T)$ to simulate the relaxation rate, least-squares fitting gives $\tau_0 = 1.20 \times 10^{-23} \text{ s}$ and $\Delta / k_B = 84.9 \text{ K}$ (inset of Figure 11). The relaxation time is located beyond the normal range for typical SCMs (usually $>10^{-12} \text{ s}$). On the other hand, the frequency

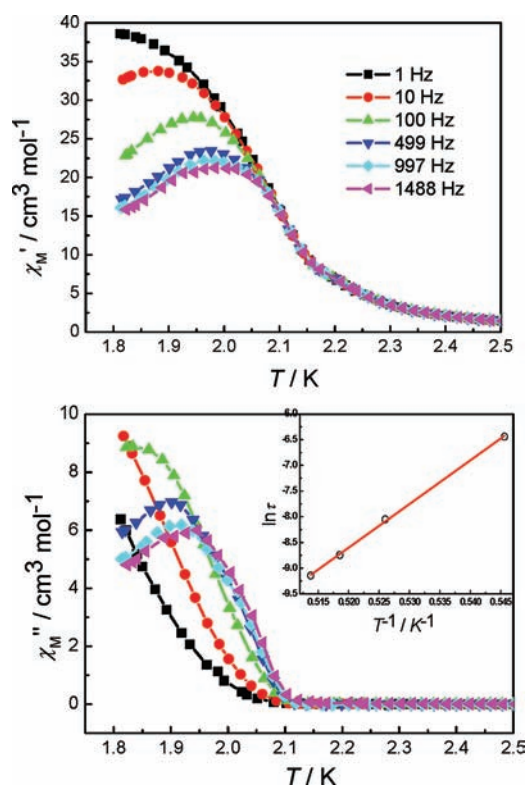


Figure 11. Temperature dependence of the in-phase χ' and out-of-phase χ'' at different frequencies for **3**. The inset is the Arrhenius fit for the $\ln \tau$ vs T^{-1} plot. The red solid line represents the best fits of the data.

dependent maxima in χ_M'' , often taken as a sign of a spin glass system, are also fitted to the dynamical slowing down for spin glasses expressed as $\tau = \tau_0 [(T_p - T_f)/T_f]^{-z\nu}$,³⁷ where τ is the relaxation time, T_f the freezing temperature, T_p the spin glass temperature, and $z\nu$ the critical exponent. The fitting results give the parameters $\tau_0 = 2.60 \times 10^{-9}$ s, $T_f = 1.43$ K, and $z\nu = 10.63$ (Supporting Information, Figure S9). The value of $z\nu$ is in the range of various spin glasses from 4 to 12. Furthermore, the plots of χ_M' , χ_M'' vs frequency at 2.0 K give a relatively large fitted α value of 0.49 (Supporting Information, Figure S10).³⁸ All ac magnetic measurements and deduced results suggest the canonical spin glasses for **3**, which may be ascribed to the single-ion anisotropy, or interchain magnetic interactions (dipolar or exchange coupling). Similar behavior was found in other 1D chain complexes, such as $[\text{Fe}(\text{qcq})(\text{CN})_3][\text{Mn}(\text{salen})] \cdot \text{MeCN} \cdot \text{H}_2\text{O}$ and $[\text{Mn}^{\text{III}}\text{TBrPP}][\text{TCNE}]$.^{29e,39}

Complexes **4** and **3** show the same magnetic behavior (Supporting Information, Figures S11–S14). The structures of enantiomers **3** and **4** are similar to those of enantiomers **1** and **2**, but their magnetic properties are obviously different. The weak interchain interactions may account for the quite different magnetic properties at low temperatures for complexes **1–4**.

CONCLUSION

In summary, with the use of $[(\text{Tp})\text{Cr}(\text{CN})_3]^-$ as the building block, four pure chiral cyano-bridged $\text{Cr}^{\text{III}}-\text{Mn}^{\text{III}}$ heterobimetallic 1D chain complexes have been synthesized and structurally characterized. Complexes **1** and **2**, and complexes **3** and **4**, are pairs of enantiomers, respectively, confirmed by circular dichroism measurements. Magnetic studies demonstrate that complexes **1** and **2** are ferrimagnets with the

magnetic transition temperature of 3.8 K, while complexes **3** and **4** show frequency-dependent ac magnetic susceptibility below 2.1 K because of the spin-glass behavior. Further research on chiral cyano-bridged bimetallic systems with interesting magnetic properties is underway in our laboratory.

ASSOCIATED CONTENT

Supporting Information

Additional structure and magnetic characterization data, and X-ray crystallographic files in CIF format for **1–4**. This material is available free of charge via the Internet at <http://pubs.acs.org>.

AUTHOR INFORMATION

Corresponding Author

*E-mail: zuojl@nju.edu.cn. Fax: +86-25-83314502.

Notes

The authors declare no competing financial interest.

ACKNOWLEDGMENTS

This work was supported by the Major State Basic Research Development Program (2011CB808704), the National Science Fund for Distinguished Young Scholars of China (20725104), and the National Natural Science Foundation of China (21021062 and 91022031). We also thank Dr. Tian-Wei Wang for experimental assistance on magnetic measurements, and Dr. Cai-Feng Wang and Zhi-Guo Gu for useful discussions.

REFERENCES

- (a) Turnbull, M. M.; Sugimoto, T.; Thompson, L. K. *Molecule-Based Magnetic Materials*; American Chemical Society: Washington, DC, 1996. (b) Miller, J. S.; Gatteschi, D. *Chem. Soc. Rev.* **2011**, *40*, 3065. (c) Mannini, M.; Pineider, F.; Saictavit, P.; Danieli, C.; Otero, E.; Sciancalepore, C.; Talarico, A. M.; Arrio, M.-A.; Cornia, A.; Gatteschi, D.; Sessoli, D. *Nat. Mater.* **2009**, *8*, 194. (d) Mannini, M.; Pineider, F.; Danieli, C.; Totti, F.; Sorace, L.; Sainctavit, P.; Arrio, M.-A.; Otero, E.; Joly, L.; Cezar, J. C.; Cornia, A.; Sessoli, R. *Nature* **2010**, *468*, 417.
- (a) Chin, J.; Lee, S. S.; Lee, K. J.; Park, S.; Kim, D. H. *Nature* **1999**, *401*, 254. (b) Train, C.; Gheorghe, R.; Krstic, V.; Chamoreau, L.-M.; Ovanesyan, N. S.; Rikken, G. L. J. A.; Gruselle, M.; Verdaguer, M. *Nat. Mater.* **2008**, *7*, 729. (c) Barron, L. D. *Nat. Mater.* **2008**, *7*, 691. (d) Train, C.; Gruselle, M.; Verdaguer, M. *Chem. Soc. Rev.* **2011**, *40*, 3297.
- (a) Rikken, G. L. J. A.; Raupach, E. *Nature* **1997**, *390*, 493. (b) Ezuhara, T.; Endo, K.; Aoyama, Y. *J. Am. Chem. Soc.* **1999**, *121*, 3279. (c) Bogani, L.; Cavigli, L.; Bernot, K.; Sessoli, R.; Gurioli, M.; Gatteschi, D. *J. Mater. Chem.* **2006**, *16*, 2587. (d) Hoshino, N.; Sekine, Y.; Nihei, M.; Oshio, H. *Chem. Commun.* **2010**, 6117.
- (a) Kaneko, W.; Kitagawa, S.; Ohba, M. *J. Am. Chem. Soc.* **2007**, *129*, 248. (b) Xiao, D. R.; Zhang, G. J.; Liu, J. L.; Fan, L. L.; Yuan, R.; Tong, M. L. *Dalton. Trans.* **2011**, 5680. (c) Fan, L. L.; Guo, F. S.; Yuan, L.; Lin, Z. J.; Herchel, R.; Leng, J. D.; Ou, Y. G.; Tong, M. L. *Dalton. Trans.* **2010**, 1771. (d) Clemente-León, M.; Coronado, E.; Dias, J. C.; Soriano-Portillo, A.; Willett, R. D. *Inorg. Chem.* **2008**, *47*, 6458. (e) Zhu, Y. Y.; Guo, X.; Cui, C.; Wang, B. W.; Wang, Z. M.; Gao, S. *Chem. Commun.* **2011**, 8049.
- (a) Gruselle, M.; Train, C.; Boubekour, K.; Gredin, P.; Ovanesyan, N. *Coord. Chem. Rev.* **2006**, *250*, 2491. (b) Liu, C. M.; Xiong, R. G.; Zhang, D. Q.; Zhu, D. B. *J. Am. Chem. Soc.* **2010**, *132*, 4044. (c) Zhang, Y. Z.; Sato, O. *Inorg. Chem.* **2010**, *49*, 1271.
- (a) Knmagai, H.; Inoue, K. *Angew. Chem., Int. Ed.* **1999**, *38*, 1601. (b) Zheng, Y.; Kong, X. J.; Long, L. S.; Huang, R. B.; Zheng, L. S. *Dalton. Trans.* **2011**, 4035. (c) Shiga, T.; Newton, G. N.; Mathieson, J. S.; Tetsuka, T.; Nihei, M.; Cronin, L.; Oshio, H. *Dalton. Trans.* **2010**, 4730.

- (7) (a) Gao, E. Q.; Yue, Y. F.; Bai, S. Q.; He, Z.; Yan, C. H. *J. Am. Chem. Soc.* **2004**, *126*, 1419. (b) Gu, Z. G.; Song, Y.; Zuo, J. L.; You, X. Z. *Inorg. Chem.* **2007**, *46*, 9522. (c) Zeng, M. H.; Wang, B.; Wang, X. Y.; Zhang, W. X.; Chen, X. M.; Gao, S. *Inorg. Chem.* **2006**, *45*, 7069.
- (8) (a) Wen, H. R.; Wang, C. F.; Li, Y. Z.; Zuo, J. L.; Song, Y.; You, X. Z. *Inorg. Chem.* **2006**, *45*, 7032. (b) Imai, H.; Inoue, K.; Kikuchi, K.; Yoshida, Y.; Ito, M.; Sunahara, T.; Onaka, S. *Angew. Chem., Int. Ed.* **2004**, *43*, 5618. (c) Inoue, K.; Kikuchi, K.; Ohba, M.; Okawa, H. *Angew. Chem., Int. Ed.* **2003**, *42*, 4810. (d) Minguet, M.; Luneau, D.; Lhotel, E.; Villar, V.; Paulsen, C.; Amabilino, D. B.; Veciana, J. *Angew. Chem., Int. Ed.* **2002**, *41*, 586. (e) Coronado, E.; Gómez-García, C. J.; Nuez, A.; Romero, F. M.; Waerenborgh, J. C. *Chem. Mater.* **2006**, *18*, 2670. (f) Akita-Tanaka, M.; Knmagai, H.; Markosyan, A.; Inoue, K. *Bull. Chem. Soc. Jpn.* **2007**, *80*, 204. (g) Numata, Y.; Inoue, K. *Chem. Lett.* **2007**, *36*, 534. (h) Armentano, D.; De Munno, G.; Lloret, F.; Palii, A. V.; Julve, M. *Inorg. Chem.* **2002**, *41*, 2007.
- (9) (a) Glauber, R. J. *J. Math. Phys.* **1963**, *4*, 294. (b) Bogani, L.; Sessoli, R.; Pini, M. G.; Rettori, A.; Novak, M. A.; Rosa, P.; Massi, M.; Fedi, M. E.; Giuntini, L.; Caneschi, A.; Gatteschi, D. *Phys. Rev. B: Condens. Matter Mater. Phys.* **2005**, *72*, 64406. (c) Caneschi, A.; Gatteschi, D.; Lalioti, N.; Sangregorio, C.; Sessoli, R.; Venturi, G.; Vindigni, A.; Rettori, A.; Pini, M. G.; Novak, M. A. *Europhys. Lett.* **2002**, *58*, 771.
- (10) (a) Coulon, C.; Miyasaka, H.; Clérac, R. *Struct. Bonding (Berlin)* **2006**, *122*, 163 and references therein. (b) Bogani, L.; Vindigni, A.; Sessoli, R.; Gatteschi, D. *J. Mater. Chem.* **2008**, *18*, 4750 and references therein. (c) Bogani, L.; Caneschi, A.; Fedi, M.; Gatteschi, D.; Massi, M.; Novak, M. A.; Pini, M. G.; Rettori, A.; Sessoli, R.; Vindigni, A. *Phys. Rev. Lett.* **2004**, *92*, 207204. (d) Miyasaka, H.; Julve, M.; Yamashita, M.; Clérac, R. *Inorg. Chem.* **2009**, *48*, 3420 and references therein. (e) Sun, H. L.; Wang, Z. M.; Gao, S. *Coord. Chem. Rev.* **2010**, *254*, 1081.
- (11) (a) Bai, Y. L.; Tao, J.; Wernsdorfer, W.; Sato, O.; Huang, R. B.; Zheng, L. S. *J. Am. Chem. Soc.* **2006**, *128*, 16428. (b) Wang, C. F.; Li, D. P.; Chen, X.; Li, X. M.; Li, Y. Z.; Zuo, J. L.; You, X. Z. *Chem. Commun.* **2009**, 6940. (c) Pardo, E.; Train, C.; Lescouëzec, R.; Journaux, Y.; Pasán, J.; Ruiz-Pérez, C.; Delgado, F. S.; Ruiz-García, R.; Lloret, F.; Paulsen, C. *Chem. Commun.* **2010**, 2322.
- (12) (a) Gerbier, P.; Domingo, N.; Gomez-Segura, J.; Ruiz-Molina, D.; Amabilino, D. B.; Tejada, J.; Williamson, B. E.; Veciana, J. *J. Mater. Chem.* **2004**, *14*, 2455. (b) Zaleski, C. M.; Depperman, E. C.; Kampf, J. W.; Kirk, M. L.; Pecoraro, V. L. *Inorg. Chem.* **2006**, *45*, 10022.
- (13) (a) Li, Y.; Xiang, S.; Sheng, T.; Zhang, J.; Hu, S.; Fu, R.; Huang, X.; Wu, X. *Inorg. Chem.* **2006**, *45*, 6577. (b) Zhang, Z. M.; Li, Y. G.; Yao, S.; Wang, E. B.; Wang, Y. H.; Clérac, R. *Angew. Chem., Int. Ed.* **2009**, *48*, 1581. (c) Singh, R.; Banerjee, A.; Colacio, E.; Rajak, K. K. *Inorg. Chem.* **2009**, *48*, 4573. (d) Sayre, H.; Milos, K.; Goldcamp, M. J.; Schroll, C. A.; Krause, J. A.; Baldwin, M. J. *Inorg. Chem.* **2010**, *49*, 4433.
- (14) (a) Mamula, O.; Lama, M.; Telfer, S. G.; Nakamura, A.; Kuroda, R.; Stoekli-Evans, H.; Scopelitti, R. *Angew. Chem., Int. Ed.* **2005**, *44*, 2527. (b) Kato, N.; Mita, T.; Kanai, M.; Therrien, B.; Kawano, M.; Yamaguchi, K.; Danjo, H.; Sei, Y.; Sato, A.; Furusho, S.; Shibasaki, M. *J. Am. Chem. Soc.* **2006**, *128*, 6768. (c) Tang, X. L.; Wang, W. H.; Dou, W.; Jiang, J.; Liu, W. S.; Qin, W. W.; Zhang, G. L.; Zhang, H. R.; Yu, K. B.; Zheng, L. M. *Angew. Chem., Int. Ed.* **2009**, *48*, 3499. (d) Kong, X. J.; Wu, Y.; Long, L. S.; Zheng, L. S.; Zheng, Z. *J. Am. Chem. Soc.* **2009**, *131*, 6918.
- (15) Milon, J.; Daniel, M. C.; Kaiba, A.; Guionneau, P.; Brandès, S.; Sutter, J. P. *J. Am. Chem. Soc.* **2007**, *129*, 13872.
- (16) (a) Coronado, E.; Gómez-García, C. J.; Nuez, A.; Romero, F. M.; Rusanov, E.; Stoekli-Evans, H. *Inorg. Chem.* **2002**, *41*, 4615. (b) Inoue, K.; Imai, H.; Ghalsasi, P. S.; Kikuchi, K.; Ohba, M.; Okawa, H.; Yakhmi, J. V. *Angew. Chem., Int. Ed.* **2001**, *40*, 4242. (c) Inoue, K.; Kikuchi, K.; Ohba, M.; Okawa, H. *Angew. Chem., Int. Ed.* **2003**, *42*, 4709.
- (17) (a) Dunbar, K. R.; Heintz, R. A. *Prog. Inorg. Chem.* **1997**, *45*, 283. (b) Weihe, H.; Güdel, H. U. *Comments Inorg. Chem.* **2000**, *22*, 75. (c) Miller, J. S. *MRS. Bull.* **2000**, *25*, 60. (d) Marvaud, V.; Decroix, C.; Scullier, A.; Guyard Duhayon, C.; Vaissermann, J.; Gonnet, F.; Verdaguer, M. *Chem.—Eur. J.* **2003**, *9*, 1677. (e) Marvaud, V.; Decroix, C.; Scullier, A.; Tuyéras, F.; Guyard-Duhayon, C.; Vaissermann, J.; Marrot, J.; Gonnet, F.; Verdaguer, M. *Chem.—Eur. J.* **2003**, *9*, 1692. (f) Wang, S.; Zuo, J. L.; Zhou, H. C.; Choi, H. J.; Ke, Y. X.; Long, J. F.; You, X. Z. *Angew. Chem., Int. Ed.* **2004**, *43*, 5940. (g) Li, D. F.; Parkin, S.; Wang, G. B.; Yee, G. T.; Clérac, R.; Wernsdorfer, W.; Holmes, S. M. *J. Am. Chem. Soc.* **2006**, *128*, 4214. (h) Li, D. F.; Parkin, S.; Wang, G. B.; Yee, G. T.; Holmes, S. M. *Inorg. Chem.* **2006**, *45*, 2773.
- (18) Beltran, L. M. C.; Long, J. R. *Acc. Chem. Res.* **2005**, *38*, 325.
- (19) Wang, C. F.; Gu, Z. G.; Lu, X. M.; Li, X. M.; Zuo, J. L.; You, X. Z. *Inorg. Chem.* **2008**, *47*, 7957.
- (20) (a) Harris, T. D.; Long, J. R. *Chem. Commun.* **2007**, 1360. (b) Yao, M. X.; Wei, Z. Y.; Gu, Z. G.; Zheng, Q.; Xu, Y.; Zuo, J. L. *Inorg. Chem.* **2011**, 21.
- (21) (a) Lescouëzec, R.; Lloret, F.; Julve, M.; Vaissermann, J.; Verdaguer, M.; Llusar, R.; Uriel, S. *Inorg. Chem.* **2001**, *40*, 2065. (b) Toma, L.; Lescouëzec, R.; Vaissermann, J.; Delgado, F. S.; Ruiz-Pérez, C.; Carrasco, R.; Cano, J.; Lloret, F.; Julve, M. *Chem.—Eur. J.* **2004**, *10*, 6130. (c) Zhang, Y. Z.; Gao, S.; Sun, H. L.; Su, G.; Wang, Z. M.; Zhang, S. W. *Chem. Commun.* **2004**, 1906.
- (22) (a) Kennedy, B. J.; Murray, K. S. *Inorg. Chem.* **1985**, *24*, 1552. (b) Miyasaka, H.; Saitoh, A.; Abe, S. *Coord. Chem. Rev.* **2007**, *251*, 2622.
- (23) Pfeifer, P.; Hesse, T.; Pfitzner, H.; Scholl, W.; Thielert, H. J. *Pract. Chem.* **1937**, *149*, 217.
- (24) Przychodzeń, P.; Lewiński, K.; Balanda, M.; Pelka, R.; Rams, M.; Wasiatyński, T.; Guyard-Duhayon, C.; Sieklucka, B. *Inorg. Chem.* **2004**, *43*, 2967.
- (25) SAINT-Plus, version 6.02; Bruker Analytical X-ray System: Madison, WI, 1999.
- (26) Sheldrick, G. M. *SADABS, An empirical absorption correction program*; Bruker Analytical X-ray Systems: Madison, WI, 1996.
- (27) Sheldrick, G. M. *SHELXL-97*; Universität of Göttingen: Göttingen, Germany, 1997.
- (28) (a) Ni, Z. H.; Zheng, L.; Zhang, L. F.; Cui, A. L.; Ni, W. W.; Zhao, C. C.; Kou, H. Z. *Eur. J. Inorg. Chem.* **2007**, 1240. (b) Kou, H. Z.; Ni, Z. H.; Liu, C. M.; Zhang, D. Q.; Cui, A. L. *New J. Chem.* **2009**, *33*, 2296. (c) Visinescu, D.; Tom, L. M.; Lloret, F.; Fabelo, O.; Pérez, C. R.; Julve, M. *Dalton Trans.* **2008**, 4103. (d) Zhang, D. P.; Wang, H. L.; Chen, Y. T.; Zhang, L. F.; Tian, L. J.; Ni, Z. H.; Jiang, J. Z. *Dalton Trans.* **2009**, 9418. (e) Wang, S.; Ferbinteanu, M.; Yamashita, M. *Inorg. Chem.* **2007**, *46*, 610.
- (29) (a) Kwak, H. Y.; Ryu, D. W.; Lee, J. W.; Yoon, J. H.; Kim, H. C.; Koh, E. K.; Krinsky, J.; Hong, C. S. *Inorg. Chem.* **2010**, *49*, 4632. (b) Yang, C.; Wang, Q. L.; Qi, J.; Ma, Y.; Yan, S. P.; Yang, G. M.; Cheng, P.; Liao, D. Z. *Inorg. Chem.* **2011**, *50*, 4006. (c) Kim, J. I.; Yoo, H. S.; Koh, E. K.; Kim, H. C.; Hong, C. S. *Inorg. Chem.* **2007**, *46*, 8481. (d) Kim, J. I.; Yoo, H. S.; Koh, E. K.; Hong, C. S. *Inorg. Chem.* **2007**, *46*, 10461. (e) Kim, J. I.; Kwak, H. Y.; Yoon, J. H.; Ryu, D. W.; Yoo, I. Y.; Yang, N.; Cho, B. K.; Park, J. G.; Lee, H.; Hong, C. S. *Inorg. Chem.* **2009**, *48*, 2956. (f) Choi, S. W.; Ryu, D. W.; Lee, J. W.; Yoon, J. H.; Kim, H. C.; Lee, H.; Cho, B. K.; Hong, C. S. *Inorg. Chem.* **2009**, *48*, 9066. (g) Yoo, H. S.; Ko, H. H.; Ryu, D. W.; Lee, J. W.; Yoon, J. H.; Lee, W. R.; Kim, H. C.; Koh, E. K.; Hong, C. S. *Inorg. Chem.* **2009**, *48*, 5617. (h) Pan, F.; Wang, Z. M.; Gao, S. *Inorg. Chem.* **2007**, *46*, 10221.
- (30) (a) Choi, H. J.; Sokol, J. J.; Long, J. R. *Inorg. Chem.* **2004**, *43*, 1606. (b) Choi, H. J.; Sokol, J. J.; Long, J. R. *J. Phys. Chem. Solids* **2004**, *65*, 839. (c) Clemente-León, M.; Coronado, E.; Giménez-López, M. C.; Soriano-Portillo, A.; Waerenborgh, J. C.; Delgado, F. S.; Ruiz-Pérez, C. *Inorg. Chem.* **2008**, *47*, 9111. (d) Miyasaka, H.; Takahashi, H.; Madanbashi, T.; Sugiura, K.-I.; Clérac, R.; Nojiri, H. *Inorg. Chem.* **2005**, *44*, 5969.
- (31) Kahn, O. *Molecular Magnetism*; VCH: Weinheim, Germany, 1993.
- (32) (a) Broderick, W. E.; Thompson, J. A.; Day, E. P.; Hoffman, B. M. *Science* **1990**, *249*, 401. (b) Kahn, O.; Pei, Y.; Verdaguer, M.; Renard, J. P.; Sletten, J. *J. Am. Chem. Soc.* **1988**, *110*, 782. (c) Nakatani, K.; Carriat, J. Y.; Journaux, Y.; Kahn, O.; Lloret, F.; Renard, J. P.; Pei, Y.; Sletten, J.; Verdaguer, M. *J. Am. Chem. Soc.* **1989**, *111*, 5739.

(d) Pei, Y.; Kahn, O.; Nakatani, K.; Codjovi, E.; Mathoniere, C.; Sletten, J. *J. Am. Chem. Soc.* **1991**, *113*, 6558. (e) Turner, S.; Kahn, O.; Rabardel, L. *J. Am. Chem. Soc.* **1996**, *118*, 6428. (f) Caneschi, A.; Gatteschi, D.; Rey, P.; Sessoli, R. *Inorg. Chem.* **1988**, *27*, 1756. (g) Caneschi, A.; Gatteschi, D.; Renard, J. P.; Rey, P.; Sessoli, R. *Inorg. Chem.* **1989**, *28*, 2940. (h) Yuan, M.; Zhao, F.; Zhang, W.; Pan, F.; Wang, Z. M.; Gao, S. *Chem.—Eur. J.* **2007**, *13*, 2937. (i) Liu, C. M.; Zhang, D. Q.; Zhu, D. B. *Inorg. Chem.* **2009**, *48*, 4980.

(33) Wen, H.-R.; Tang, Y.-Z.; Liu, C.-M.; Chen, J.-L.; Yu, C.-L. *Inorg. Chem.* **2009**, *48*, 10177.

(34) (a) Ni, Z.-H.; Tao, J.; Wernsdorfer, W.; Cui, A.-L.; Kou, H.-Z. *Dalton Trans.* **2009**, 2788. (b) Miyasaka, H.; Ieda, H.; Matsumoto, N.; Re, N.; Crescenzi, R.; Floriani, C. *Inorg. Chem.* **1998**, *37*, 255. (c) Miyasaka, H.; Matsumoto, N.; Okawa, H.; Re, N.; Gallo, E.; Floriani, C. *J. Am. Chem. Soc.* **1996**, *118*, 981. (d) Ferbinteanu, M.; Miyasaka, H.; Wernsdorfer, W.; Nakata, K.; Sugiura, K.; Yamashita, M.; Coulon, C.; Clérac, R. *J. Am. Chem. Soc.* **2005**, *127*, 3090. (e) Re, N.; Gallo, E.; Floriani, C.; Miyasaka, H.; Matsumoto, N. *Inorg. Chem.* **1996**, *35*, 6004. (f) Ni, Z.-H.; Kou, H.-Z.; Zhang, L.-F.; Ge, C.; Cui, A.-L.; Wang, R.-J.; Li, Y.; Sato, O. *Angew. Chem., Int. Ed.* **2005**, *44*, 7742. (g) Ni, Z.-H.; Zhang, L.-F.; Tangoulis, V.; Wernsdorfer, W.; Cui, A.-L.; Sato, O.; Kou, H.-Z. *Inorg. Chem.* **2007**, *46*, 6029. (h) Ni, W.-W.; Ni, Z.-H.; Cui, A.-L.; Liang, X.; Kou, H.-Z. *Inorg. Chem.* **2007**, *46*, 22.

(35) Zhang, D. P.; Wang, H. L.; Chen, Y. T.; Ni, Z.-H.; Tian, L. J.; Jiang, J. Z. *Inorg. Chem.* **2009**, *48*, 11215.

(36) Mydosh, J. A. *Spin glasses: An Experimental Introduction*; Taylor & Francis: London, U.K., 1993.

(37) (a) Zheng, Y.-Z.; Tong, M.-L.; Zhang, W.-X.; Chen, X.-M. *Angew. Chem., Int. Ed.* **2006**, *45*, 6310. (b) Li, X.-J.; Wang, X.-Y.; Gao, S.; Cao, R. *Inorg. Chem.* **2006**, *45*, 1508.

(38) (a) Aubin, S. M. J.; Sun, Z.; Pardi, L.; Krzystek, J.; Folting, K.; Brunel, L.-C.; Rheingold, A. L.; Christou, G.; Hendrickson, D. N. *Inorg. Chem.* **1999**, *38*, 5329. (b) Wang, Z.-X.; Li, X.-L.; Wang, T.-W.; Li, Y.-Z.; Ohkoshi, S.; Hashimoto, K.; Song, Y.; You, X.-Z. *Inorg. Chem.* **2007**, *46*, 10990.

(39) Rittenberg, D. K.; Sugiura, K.-i.; Sakata, Y.; Mikami, S.; Epstein, A. J.; Miller, J. S. *Adv. Mater.* **2000**, *12*, 126.